
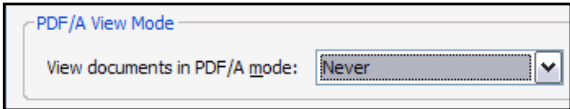
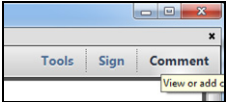
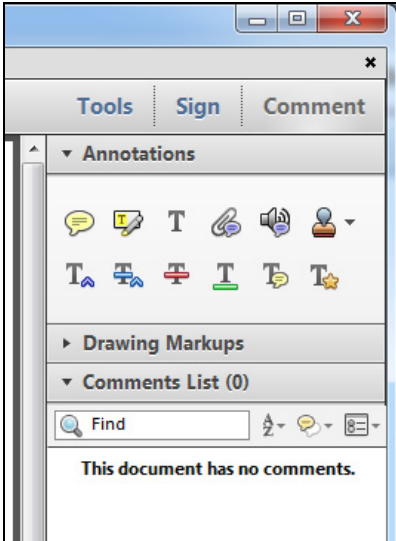


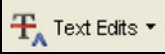


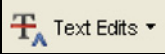

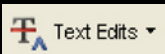





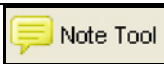

INSTRUCTIONS ON THE ANNOTATION OF PDF FILES

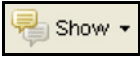
To view, print and annotate your article you will need Adobe Reader version 9 (or higher). This program is freely available for a whole series of platforms that include PC, Mac, and UNIX and can be downloaded from <http://get.adobe.com/reader/>. The exact system requirements are given at the Adobe site: <http://www.adobe.com/products/reader/tech-specs.html>.

Note: if you opt to annotate the file with software other than Adobe Reader then please also highlight the appropriate place in the PDF file.

PDF ANNOTATIONS	
Adobe Reader version 9	Adobe Reader version X and XI
<p>When you open the PDF file using Adobe Reader, the Commenting tool bar should be displayed automatically; if not, click on 'Tools', select 'Comment & Markup', then click on 'Show Comment & Markup tool bar' (or 'Show Commenting bar' on the Mac). If these options are not available in your Adobe Reader menus then it is possible that your Adobe Acrobat version is lower than 9 or the PDF has not been prepared properly.</p>  <p>(Mac)</p> <p>PDF ANNOTATIONS (Adobe Reader version 9)</p> <p>The default for the Commenting tool bar is set to 'off' in version 9. To change this setting select 'Edit Preferences', then 'Documents' (at left under 'Categories'), then select the option 'Never' for 'PDF/A View Mode'.</p>  <p>(Changing the default setting, Adobe version 9)</p>	<p>To make annotations in the PDF file, open the PDF file using Adobe Reader XI, click on 'Comment'.</p> <p>If this option is not available in your Adobe Reader menus then it is possible that your Adobe Acrobat version is lower than XI or the PDF has not been prepared properly.</p>  <p>This opens a task pane and, below that, a list of all Comments in the text. These comments initially show all the changes made by our copyeditor to your file.</p> 

HOW TO...

Action	Adobe Reader version 9	Adobe Reader version X and XI
Insert text	Click the 'Text Edits' button  on the Commenting tool bar. Click to set the cursor location in the text and simply start typing. The text will appear in a commenting box. You may also cut-and-paste text from another file into the commenting box. Close the box by clicking on 'x' in the top right-hand corner.	Click the 'Insert Text' icon  on the Comment tool bar. Click to set the cursor location in the text and simply start typing. The text will appear in a commenting box. You may also cut-and-paste text from another file into the commenting box. Close the box by clicking on 'x'  in the top right-hand corner.
Replace text	Click the 'Text Edits' button  on the Commenting tool bar. To highlight the text to be replaced, click and drag the cursor over the text. Then simply type in the replacement text. The replacement text will appear in a commenting box. You may also cut-and-paste text from another file into this box. To replace formatted text (an equation for example) please Attach a file (see below).	Click the 'Replace (Ins)' icon  on the Comment tool bar. To highlight the text to be replaced, click and drag the cursor over the text. Then simply type in the replacement text. The replacement text will appear in a commenting box. You may also cut-and-paste text from another file into this box. To replace formatted text (an equation for example) please Attach a file (see below).
Remove text	Click the 'Text Edits' button  on the Commenting tool bar. Click and drag over the text to be deleted. Then press the delete button on your keyboard. The text to be deleted will then be struck through.	Click the 'Strikethrough (Del)' icon  on the Comment tool bar. Click and drag over the text to be deleted. Then press the delete button on your keyboard. The text to be deleted will then be struck through.
Highlight text/ make a comment	Click on the 'Highlight' button  on the Commenting tool bar. Click and drag over the text. To make a comment, double click on the highlighted text and simply start typing.	Click on the 'Highlight Text' icon  on the Comment tool bar. Click and drag over the text. To make a comment, double click on the highlighted text and simply start typing.
Attach a file	Click on the 'Attach a File' button  on the Commenting tool bar. Click on the figure, table or formatted text to be replaced. A window will automatically open allowing you to attach the file. To make a comment, go to 'General' in the 'Properties' window, and then 'Description'. A graphic will appear in the PDF file indicating the insertion of a file.	Click on the 'Attach File' icon  on the Comment tool bar. Click on the figure, table or formatted text to be replaced. A window will automatically open allowing you to attach the file. A graphic will appear indicating the insertion of a file.
Leave a note/ comment	Click on the 'Note Tool' button  on the Commenting tool bar. Click to set the location of the note on the document and simply start typing. <u>Do not use this feature to make text edits.</u>	Click on the 'Add Sticky Note' icon  on the Comment tool bar. Click to set the location of the note on the document and simply start typing. <u>Do not use this feature to make text edits.</u>

HOW TO...		
Action	Adobe Reader version 9	Adobe Reader version X and XI
Review	To review your changes, click on the 'Show' button  on the Commenting tool bar. Choose 'Show Comments List'. Navigate by clicking on a correction in the list. Alternatively, double click on any mark-up to open the commenting box.	Your changes will appear automatically in a list below the Comment tool bar. Navigate by clicking on a correction in the list. Alternatively, double click on any mark-up to open the commenting box.
Undo/delete change	To undo any changes made, use the right click button on your mouse (for PCs, Ctrl-Click for the Mac). Alternatively click on 'Edit' in the main Adobe menu and then 'Undo'. You can also delete edits using the right click (Ctrl-click on the Mac) and selecting 'Delete'.	To undo any changes made, use the right click button on your mouse (for PCs, Ctrl-Click for the Mac). Alternatively click on 'Edit' in the main Adobe menu and then 'Undo'. You can also delete edits using the right click (Ctrl-click on the Mac) and selecting 'Delete'.

SEND YOUR ANNOTATED PDF FILE BACK TO ELSEVIER

Save the annotations to your file and return as instructed by Elsevier. Before returning, please ensure you have answered any questions raised on the Query Form and that you have inserted all corrections: later inclusion of any subsequent corrections cannot be guaranteed.

FURTHER POINTS

- Any (grey) halftones (photographs, micrographs, etc.) are best viewed on screen, for which they are optimized, and your local printer may not be able to output the greys correctly.
- If the PDF files contain colour images, and if you do have a local colour printer available, then it will be likely that you will not be able to correctly reproduce the colours on it, as local variations can occur.
- If you print the PDF file attached, and notice some 'non-standard' output, please check if the problem is also present on screen. If the correct printer driver for your printer is not installed on your PC, the printed output will be distorted.

Semiautomated Detection and Quantification of Aortic Plaques from Three-Dimensional Transesophageal Echocardiography

Concetta Piazzese, Andy Tsang, Miguel Sotaqui, Yzhak Kronzon, Roberto M. Lang, and Enrico G. Caiani, Milan, Italy; Toronto, Ontario, Canada; New York, New York; Chicago, Illinois; Lugano, Switzerland

Background: Aortic atherosclerosis is a risk factor for cerebrovascular events. Two-dimensional transesophageal echocardiographic quantification of descending aortic plaques is time-consuming and underestimates plaque burden. The aim of this study was to assess the feasibility and accuracy of a novel semiautomated program to use three-dimensional (3D) transesophageal echocardiography to identify and quantify aortic plaque severity as determined by plaque thickness, volume, and number. The relationship between maximum plaque thickness and volume was also examined.

Methods: Descending aortic 3D transesophageal echocardiographic images from 58 patients were analyzed for plaque thickness, volume, and number using semiautomated, custom software. The reference standard was manual assessment by an expert reader using 3D multiplanar reconstructions. Agreement and κ values were calculated to determine the program's accuracy against the reference standard. Correlation and bias were examined using linear regression and Bland-Altman statistics. Pearson's correlation was used to examine the relationship between maximum plaque thickness and volume.

Results: Analysis was possible in all patients. Overall agreement for the absolute presence or absence of plaque per patient was 95%. Agreement regarding the number of plaques per patient and plaque severity was high at 95% and 85%, respectively. Plaque volume was slightly underestimated by the program compared with manual measurements. The correlation between plaque thickness and volume was 0.56.

Conclusions: The results of this study demonstrate that semiautomated plaque analysis of 3D transesophageal echocardiographic descending aortic data sets is feasible and accurate in determining plaque severity as measured by plaque thickness, volume, and number. This methodology allows the standardization of plaque quantification, which will improve its utility in clinical trials. A greater understanding of the importance of plaque thickness versus volume is needed. (J Am Soc Echocardiogr 2014; ■:■-■.)

Keywords: Aortic plaque, Three-dimensional transesophageal echocardiography

Strokes are the fourth leading cause of death in the United States, and transesophageal echocardiographic (TEE) imaging is routinely performed in patients with stroke when an extracardiac source of embolism

From the Dipartimento di Elettronica, Informazione e Bioingegneria, Politecnico di Milano, Milan, Italy (C.P., M.S., E.G.C.); University Health Network, Toronto General Hospital, University of Toronto, Toronto, Ontario, Canada (W.T.); Lenox Hill Heart and Vascular Institute of New York, New York, New York (I.K.); University of Chicago Medical Center, Chicago, Illinois (R.M.L.); Università della Svizzera Italiana, Lugano, Switzerland (E.G.C.).

Drs Piazzese and Tsang contributed equally to this work.

Dr Tsang was funded by a Canadian Institutes of Health Research Fellowship. Dr Lang received a small research grant from Philips Medical Systems (Andover, MA).

Reprint requests: Roberto M. Lang, University of Chicago Medical Center, 5841 South Maryland Avenue, MC 5084, Chicago, IL 60637 (E-mail: rlang@medicine.bsd.uchicago.edu).

0894-7317/\$36.00

Copyright 2014 by the American Society of Echocardiography.

<http://dx.doi.org/10.1016/j.echo.2014.03.003>

has not been identified.^{1,2} Typically, at the end of a TEE examination, the echocardiographer will examine the aorta for complex atherosclerotic plaques, which when present significantly increased stroke risk.³⁻⁵ To be considered complex, these plaques must be ≥ 4 mm in thickness, be ulcerated, or contain mobile thrombi. However, determination of plaque complexity from two-dimensional (2D) TEE images may be inaccurate, because only one cross-sectional plane can be visualized or measured at a time, ignoring the complex three-dimensional (3D) shape of the plaque.

Three-dimensional TEE imaging of the aorta results in the acquisition of 3D aortic plaque data sets that can be used to accurately quantify the plaque's 3D dimensions and volume. However, this quantification is a tedious and time-consuming process because it requires manual analysis of multiple 2D images from the 3D data set. We hypothesized that this process would benefit from automation and accordingly developed semiautomated software that detects and quantifies plaques from 3D descending aortic TEE images. The aim of this study was to assess the feasibility and accuracy of the program to (1) identify the presence or absence of plaque, (2) identify the locations and number of plaques, (3) determine plaque severity, (4)

Abbreviations

CT = Computed tomography

MRI = Magnetic resonance imaging

TEE = Transesophageal echocardiographic

3D = Three-dimensional

2D = Two-dimensional

determine plaque volume, and (5) determine the relationship, if any, between maximum plaque thickness and plaque volume.

METHODS

Study Protocol

Clinically indicated TEE studies were performed in 58 patients (35 men; mean age, 60 ± 16 years). Forty-one patients were studied at the University of Chicago and 17 at the Lenox Hill Heart and Vascular Institute. Three-dimensional TEE (X-7t; Philips Medical Imaging, Best, The Netherlands) data sets of the descending aorta were acquired, using single-beat, narrow-angle acquisition mode. These images were acquired at 0° , with the TEE probe rotated toward the descending aorta (Figure 1). First, the 2D short-axis image of the aorta was optimized, allowing maximum contrast between blood-tissue planes. Then, multiplane mode was used to ensure that the short axis and long axis of the aorta were centered within the 3D pyramidal volume. Finally, narrow-angle, single-beat data sets, with the acquisition pyramid minimized to include only the aorta, were acquired. Gain and rendering settings were left up to the discretion of the operators, as both sites have extensive experience acquiring 3D data sets. No postprocessing was required after acquisition.

If no atherosclerotic plaque was present, a representative region of the descending aorta was imaged. If atherosclerotic plaque was present, overlapping 3D data sets were obtained from the level of the diaphragm to the aortic arch. The descending aorta was defined as the portion that could first be imaged during withdrawal from the stomach. The aortic arch was defined where the short-axis image of the aorta could no longer be kept centered and circular during withdrawal of the probe. These data sets were then exported in Digital Imaging and Communications in Medicine format for semiautomated analysis on a dedicated computer system. The institutional review boards of both institutions approved the protocol. The software was written in Chicago and Milan.

Semiautomated Plaque Analysis

An algorithm that requires minimal user interaction for plaque segmentation and quantification was developed (see the Appendix for further details). No patent application has been made.

Three-Dimensional Data Set Orientation. The first step of the analysis was to orient the 3D volume such that one axis corresponds to the longitudinal dimension of the aorta. This was achieved by having the user define a volume of interest by selecting two slices that mark the ends of the aorta (Figure 2A) within the 3D data set. The user then selected a point in each of these slices that visually corresponded to the center of the aortic lumen. A line passing between these two points represented the long axis of the aorta. The 3D data set was then rotated so that the short-axis aortic lumen was presented, which was perpendicular to the calculated long axis. This presented view was required for the segmentation process.

True Aortic Luminal 3D Mesh. After orientation of the 3D volume of interest, an automated algorithm was applied to detect the surface of the aorta, generating a 3D mesh M (Figure 2C, in grayscale). This was performed using the marching cubes algorithm.⁶ This 3D

mesh traces the true aortic luminal surface because it includes plaques along the wall.

Ideal Aortic Lumen. Using the short-axis cut-planes, five points on the aortic wall, excluding the plaques if present, were manually selected. Assuming that the short-axis cross-section of the aortic lumen has an ellipsoidal 2D shape, an elliptical curve passing through the five manually chosen points was determined using least squares minimization criteria (see the Appendix for details). This process was repeated on seven equally spaced short-axis planes. For the planes that were not manually marked, the luminal contours were obtained by linear interpolation (Figures 2B and C). This luminal contour represents the ideal aortic lumen because aortic plaques are excluded from the surface.

Plaque Identification and Segmentation. Automated plaque detection was achieved by comparing the true 3D mesh with the ideal aortic lumen. The difference between these two lumens was presumed to be plaque. After segmentation, for each plaque, the local thickness and total internal volume were computed.

Plaque Detection. For comparison of plaque detection in terms of number and location, the 3D true luminal mesh with the detected plaques highlighted using a three-level color map (green = mild, yellow = moderate, red = severe) on the basis of their local thickness (Figure 4B) was exported for visual comparison with the manual reference standard. Plaque thickness was color coded as mild if >1 and <2 mm, moderate if between 2 and 4 mm, and severe if >4 mm.⁵

Plaque Severity Grading. For each plaque, the maximum thickness determined the semiautomated plaque severity grade using the scale described for color-coded display of plaque thickness.

Plaque Volume Computation. For each plaque, its internal volume was computed using the method of disks.

Reference Standard Analysis

An experienced cardiologist, blinded to the results of the semiautomated analysis program, used multiplanar analysis of the 3D data sets (QLAB version 9.1; Philips Medical Systems, Andover, MA) to determine the reference standard results.

Plaque Detection. To determine the number of plaques and their locations, plaques were manually identified in a systematic cranial-to-caudal direction using three orthogonal views. For each plaque, a screen shot of the rendered 3D volume and the cross-sectional cut planes that intersected the plaque was exported (Figures 4A, 4C–4E). A second independent observer then compared the semiautomated program's output with the rendered 3D volume screen shot (Figure 5).

Plaque Severity Grading. For each identified plaque, the thickest dimension was measured perpendicular to the base of the plaque. Manual measurements of maximal plaque thickness were then used to classify plaques as mild, moderate, or severe using the same scale as used to classify plaque severity with the semiautomated program.

Plaque Volume Computation. Fifteen data sets containing isolated plaques were selected for comparison of the semiautomated program-derived plaque volumes with manually measured volumes. Custom software was used to manually trace the plaques from cross-

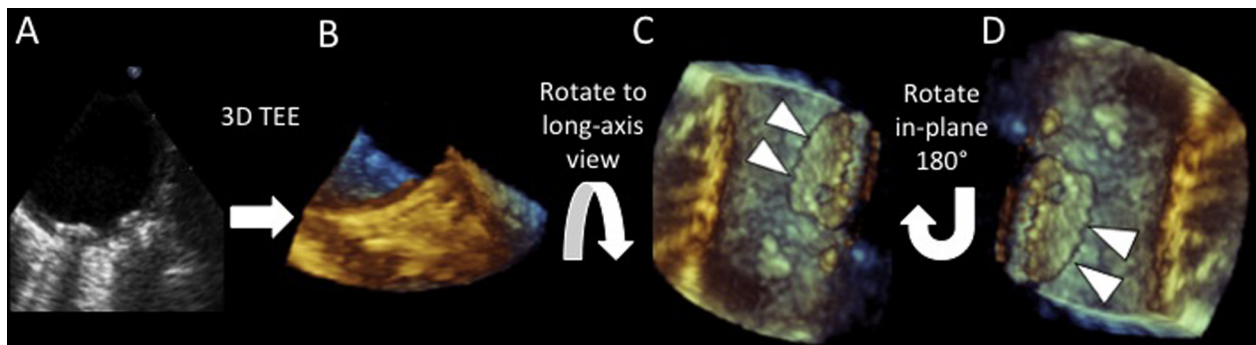


Figure 1 Three-dimensional TEE acquisition of the aorta. When a plaque was visually detected on 2D imaging (A), 3D zoom mode was activated to obtain a volumetric data set of the aorta centered on the same cross-section at a 0° transducer angle (B). This image was tilted to reveal the intimal surface of the aorta (C) and then rotated along the z axis by 180° to place the image in the correct anatomic orientation (D).

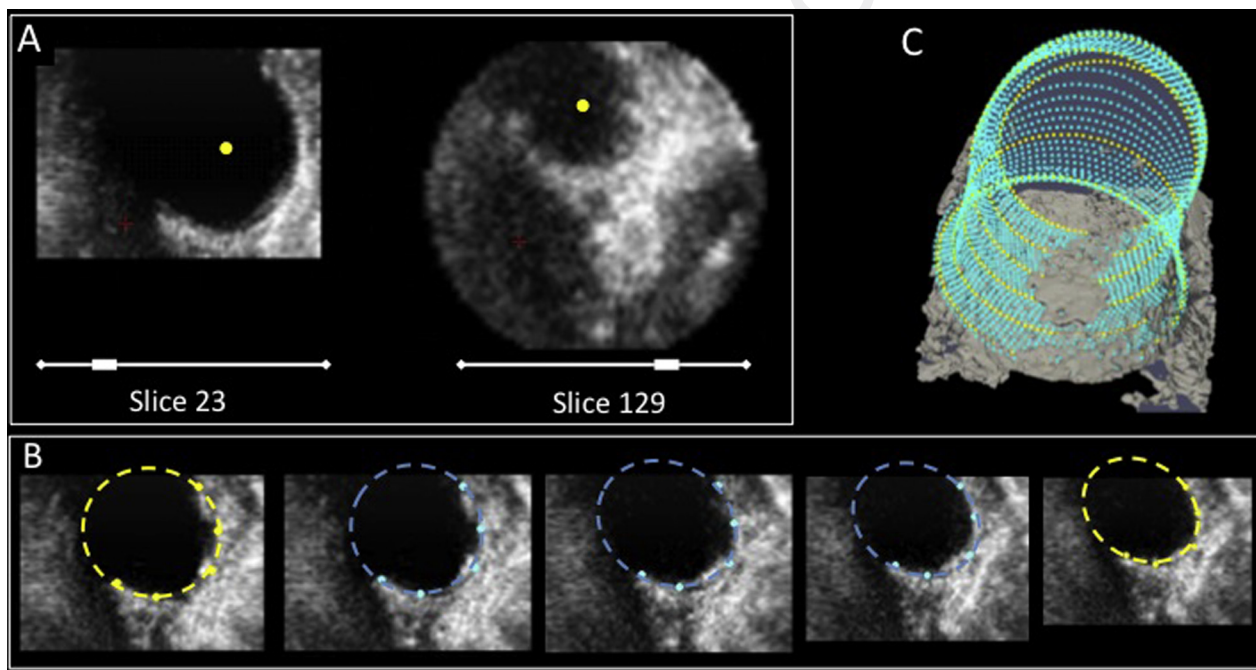


Figure 2 Semiautomated plaque analysis. To correctly align the 3D volume, the user selected one point in the first and last slices from unoriented aortic cross-sections. These points were used to compute the line passing between them and realign the 3D data set on the basis of the line's orientation (A). Manually selected points on seven evenly spaced, correctly oriented aortic cross-sections were used to determine an ideal aortic luminal contour (yellow dashed line, B). With linear interpolation of points in the cut planes between initialized cross-sections, the ideal aortic luminal contour was completed (cyan). Automated thresholding of the video-intensity data was used to create a 3D mesh (white) representing the true aortic lumen (C), which was then overlaid with the ideal luminal contour.

sectional slices. Plaque volume was calculated from these tracings using the method of disks (Figures 6A and 6B).

Statistical Analysis

Agreement and κ values were calculated to determine the software's accuracy against the gold-standard analysis with respect to (1) the presence or absence of plaque per patient, (2) the number of plaques per patient, and (3) plaque severity. Kappa analysis was performed with linear weights. Linear regression was performed to examine the correlation between the automated and manual measurements of plaque volume. As well, Bland-Altman analysis was performed to calculate potential bias with the automated volumes. Finally,

Pearson's correlation was performed to examine the relationship between maximum plaque thickness and plaque volume.

RESULTS

Analysis was possible in all patients. The maximum time for automated analysis of the 3D data sets was approximately 5 min, regardless of plaque severity. This time included data retrieval, preprocessing, and initialization. The approximate time for manual analysis of the data sets varied from 5 min in patients with simple plaques to 30 min in patients with complex plaques. Figure 4 presents

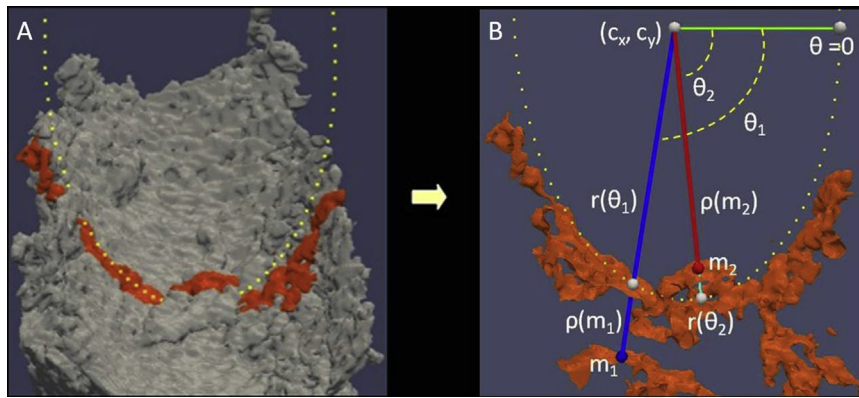


Figure 3 Automated plaque segmentation. **(A)** The 3D mesh of the aortic inner surface was visualized in gray. Highlighted in yellow were the nodes associated to the 2D n th cross-sectional cut plane corresponding to the computed elliptical luminal contour. **(B)** To determine if nodes m_1 and m_2 on the mesh were plaques, their distances $\rho(m_1)$ and $\rho(m_2)$ from the ellipse center (x_0, y_0) were computed and compared with the corresponding distances $r(\theta_1)$ and $r(\theta_2)$ of the points on the ellipse contour. By comparing these distances, node m_1 was not classified as a plaque, whereas node m_2 was classified as a plaque.

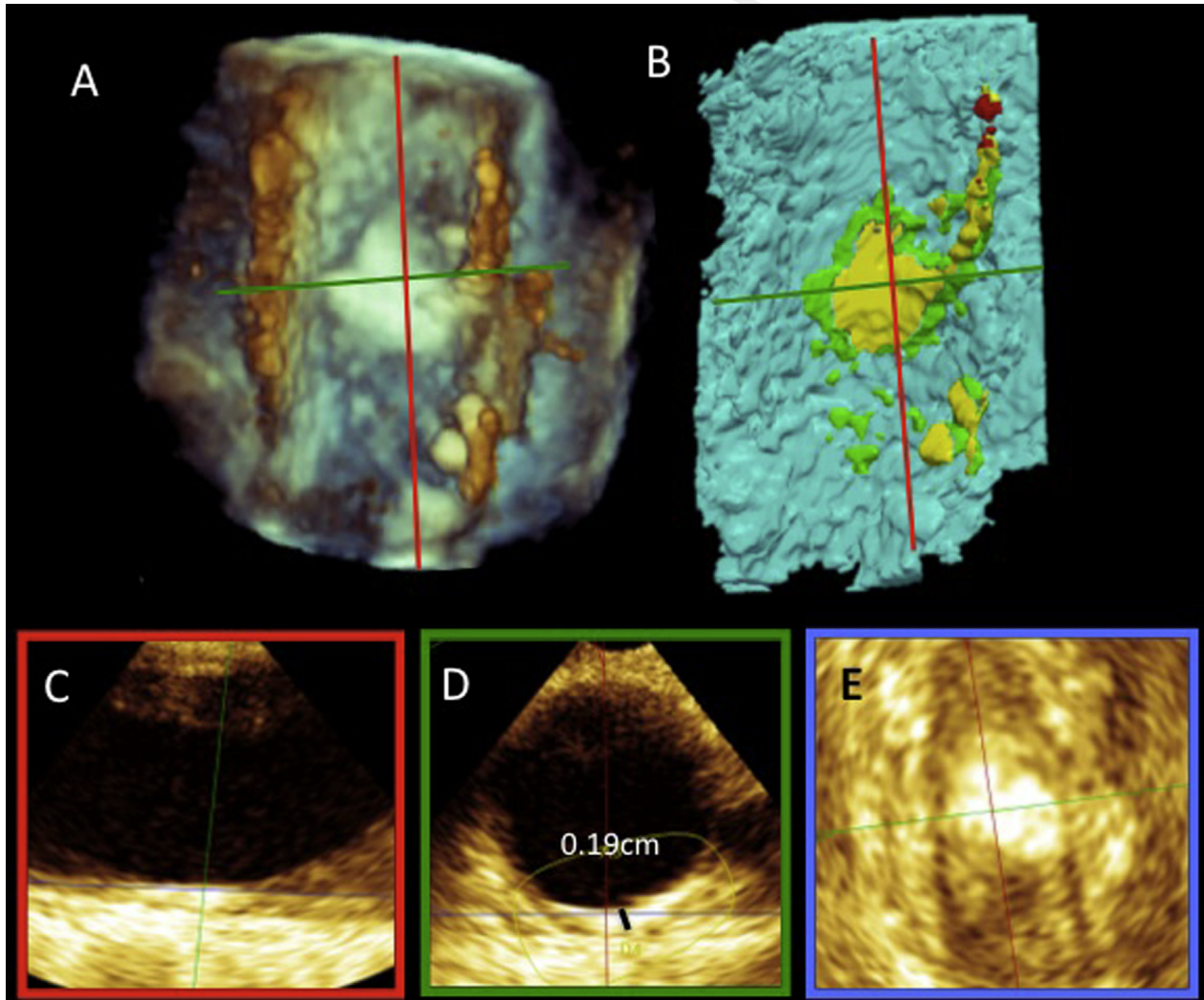


Figure 4 Data analysis. Screen shot of the rendered 3D volume **(A)** and visualizing the output of the segmentation **(B)**. Multiplanar analysis with three cut planes **(C–E)**. The red cut plane **(C)** was oriented along the long axis of the aorta and the green cut plane **(D)** along the short axis. The blue plane **(E)**, perpendicular to both the red and green planes, allowed “en face” visualization of the plaque for comparison to the automated analysis results **(B)**.

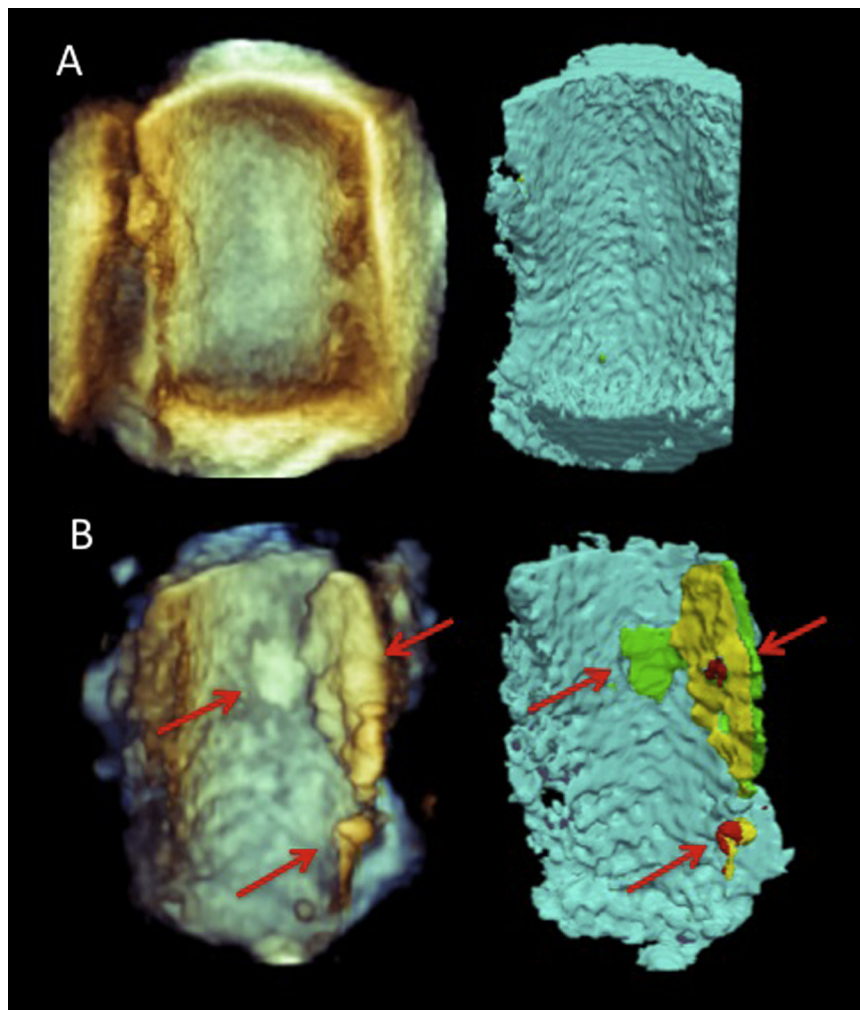


Figure 5 Example of program output. Example of a normal (**A**) and diseased (**B**) aorta as it appeared in the 3D TEE data set (*left column*) and the automated analysis software (*right column*), respectively. Red arrows point to atherosclerotic plaques.

the 3D rendered volume data with the corresponding semiautomated program output in a subject with no plaques and in a second subject with three separate plaques that were identified by both the reference standard and the software.

When we examined the semiautomated program's ability to detect the presence or absence of plaque in each patient, we found that there was agreement with the reference standard on the presence of plaque in 55 subjects and disagreement in three subjects. Thus, agreement on the absolute presence or absence of plaque per patient was 95%.

Next, we examined the semiautomated program's ability to correctly identify the locations and number of plaques in each subject. Overall, the program correctly identified and located 145 of 162 plaques (see Table 1). Thus, on a per patient basis, agreement with respect to the number of plaques was 95% ($\kappa = 0.89$).

Subsequently, we examined the accuracy of the program in identifying plaque severity. Overall, in 116 of the 145 plaques identified by the program, there was no difference in plaque severity as automatically assessed compared with manual measurement. Of the remaining 29 plaques that demonstrated changes in severity, 15 had decreases in severity by one grade, and 14 had increases in severity by one grade (Figure 7). No plaque differed by more than one grade

in severity. In terms of clinical relevance, four plaques changed from being classified as moderate by the program to severe by the reference standard analysis, and five changed from being classified as severe to being moderate. Overall, agreement between the reference standard and the software with respect to plaque severity was 80% ($\kappa = 0.64$). When we examined the maximum plaque severity per patient, the agreement between the reference standard and the software increased to 85% ($\kappa = 0.78$).

When we examined the accuracy of the program to quantify plaque volume, we found a high correlation of 0.99 between semiautomated and manual measurements of plaque volume. When examining bias, we found that the automated program slightly underestimated (bias, $-2.1 \pm 1.9 \text{ mm}^3$) compared with manual measurements.

Finally, we examined the relationship between maximum plaque thickness and plaque volume (Figure 6). The correlation between these two measurements was moderate at 0.56. When these variables were plotted, the graph demonstrated that some plaques would be considered severe, with maximum thicknesses $> 4 \text{ mm}$, yet have very low volumes. In contrast, other plaques would be considered moderate in severity, with maximum thicknesses of 2 to 4 mm, yet have large volumes.

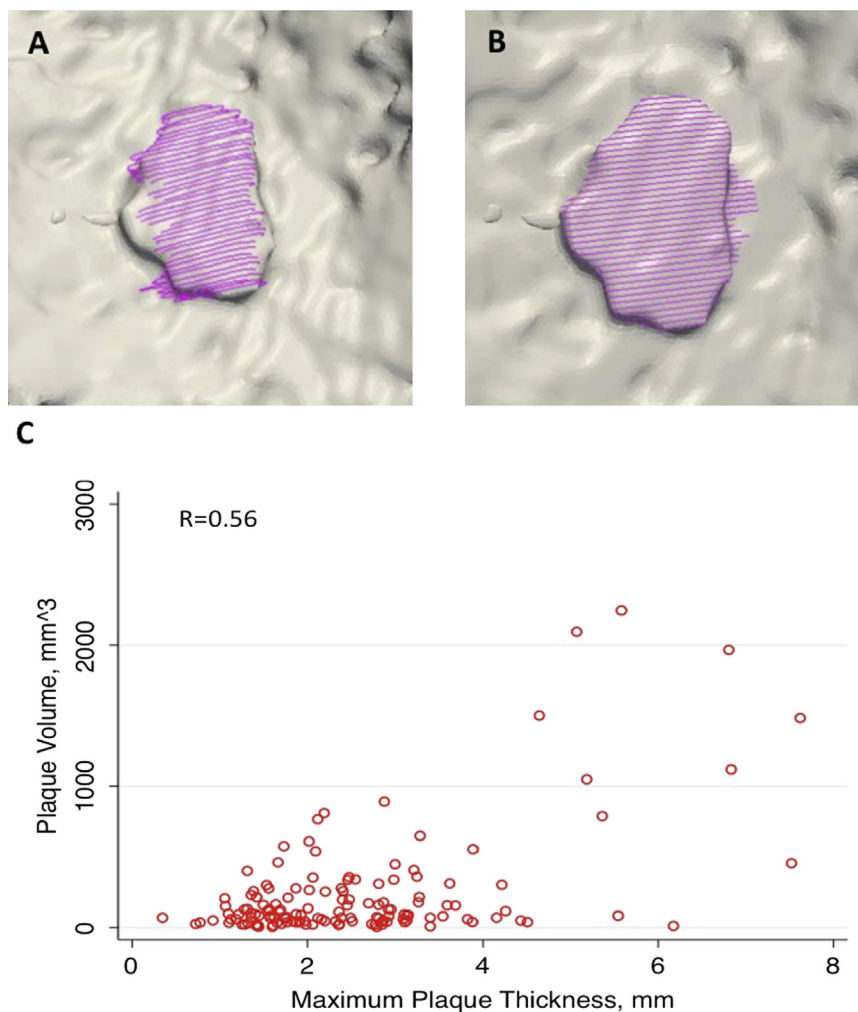


Figure 6 Measurement of plaque volume. Comparison of the contours obtained manually (A) and by the semiautomated program (B), which were then used in the computation of plaque volume by the method of disks. (C) Relationship between maximum plaque thickness and volume as determined by the automated program.

Table 1 Distribution of plaque grading on the basis of thickness by method of assessment

	Mild	Moderate	Severe	Total
Reference standard	64	89	9	162
Semiautomated	56	74	15	145
False positive	1	1	0	2
False negative	11	6	0	17

False-positive and false-negative classifications are reported by plaque severity. Plaque severity was classified as mild (>1 and <2 mm), moderate (2–4 mm), or severe (>4 mm).

DISCUSSION

This study demonstrates that semiautomated analysis of 3D TEE data sets of the descending aorta for atheromatous plaques is feasible and accurate in determining plaque presence and severity measured by plaque thickness, volume, or number. As well, we found that

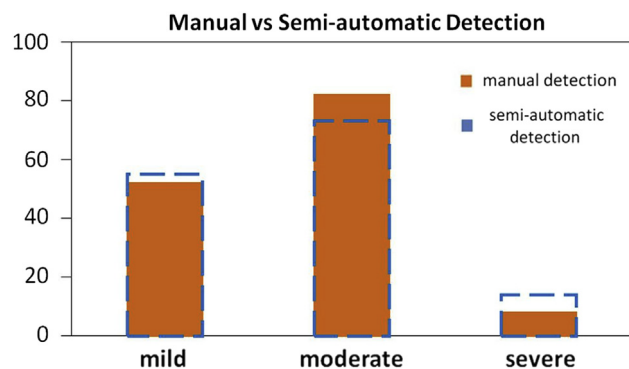


Figure 7 Manual versus semiautomated plaque detection. Differences in the classification of plaque severity for plaques that were detected by both the reference standard and the semiautomated software. Plaque severity was determined by the computed thickness (mild, >1 and <2 mm; moderate, 2–4 mm; severe, >4 mm). Differences in the bar graph represent misclassifications.

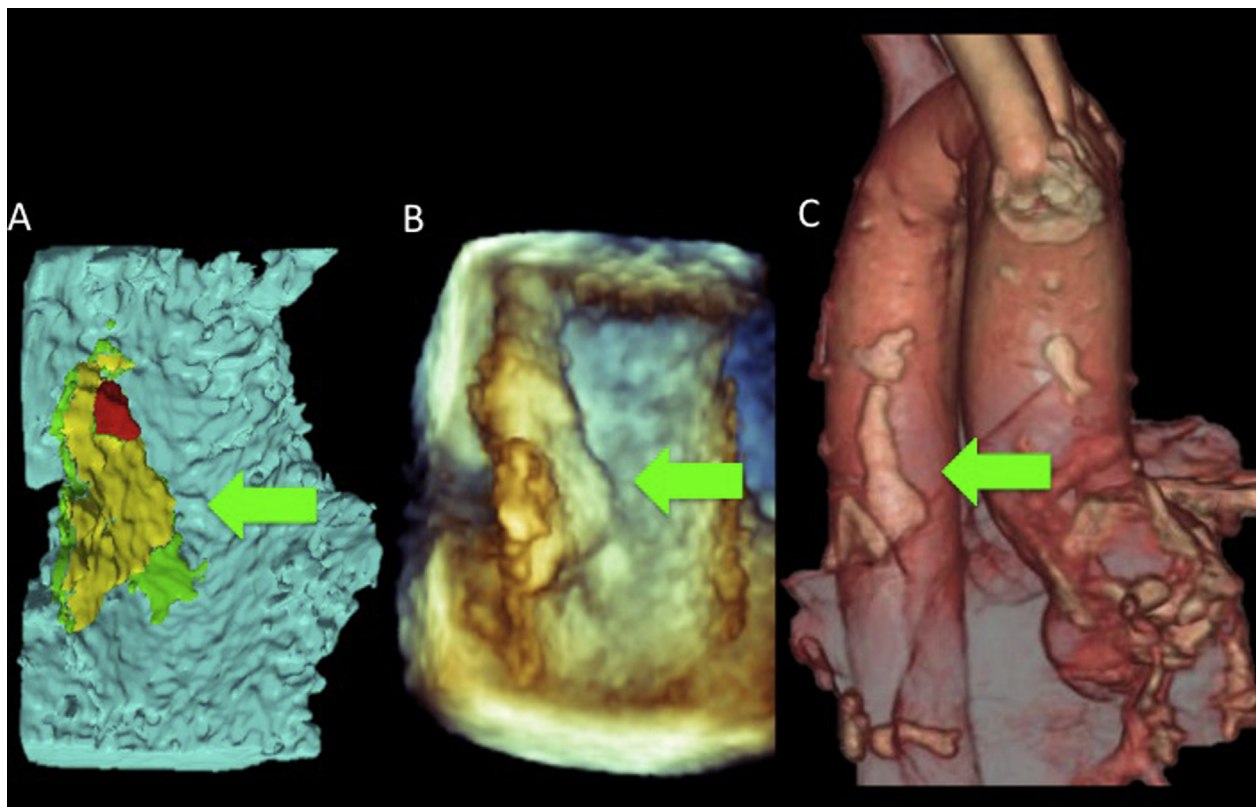


Figure 8 Example of a plaque visualized by the automated program, with severity highlighted by a three-level color map (A), the corresponding 3D rendered volumetric data (B), and on volume-rendered CT (C).

maximum plaque thickness was only moderately correlated with plaque volume.

Historically, aortic assessments for atheromatous plaques were performed using contrast angiography. However, this methodology is invasive, requires the use of contrast and radiation, and, compared with TEE imaging, misdiagnoses plaques.⁷ Thus, other methods have evolved, including magnetic resonance imaging (MRI) and computed tomography (CT). However, MRI is expensive and cannot be performed at the bedside or on patients with ferromagnetic implants, while CT exposes patients to radiation and contrast injection.

TEE imaging is readily available and is routinely performed on patients to identify cardiac sources of embolic events, as well as during cardiac surgery. As well, transesophageal echocardiography is the main imaging modality used to guide percutaneous procedures, in which complication rates are increased by periprocedural plaque embolization.⁸ Plaque visualization is similar to that seen on CT (Figure 8), so plaques identified preprocedurally on CT can be followed periprocedurally. Thus, TEE imaging is a suitable tool for assessing aortic atherosclerosis. However, it must be noted that the tracheal air column, near the origin of the innominate artery, masks a small portion of the ascending aorta, and this “blind spot” likely results in missing only approximately 2% of plaques.^{4,9,10}

Traditionally, when using 2D TEE imaging to determine plaque burden, for each plaque, the imager must manually move the probe to determine if the thickest portion of the plaque exceeds 4 mm, note if mobile components or ulcerations are present, and mentally infer the plaque’s length and width. This is not only tedious and time-consuming but may result in an inaccurate assessment. This is related to poor quantification due to plaque shape. As demonstrated

in this study, a long, thin, multilobar plaque may represent a larger burden of disease than a single small plaque that protrudes into the lumen. Three-dimensional TEE imaging allows the entire plaque morphology to be visualized, thereby allowing the true complexity of the plaque to be assessed. However, without dedicated software, plaque identification and the quantification of plaque area and thickness from 3D TEE data sets are tedious and time-consuming.

Three-dimensional multiplanar reconstruction was chosen as the reference standard for this study. This allowed direct comparison of the plaques identified by the automated program with the 3D data set. The use of 2D imaging as a reference standard would be problematic because one could never be confident that the single 2D planar image matches the plaque identified by the automated program. This is especially true when trying to confirm that the automatic program recognized the entire 3D plaque shape. This is because the single-plane views may not recognize an asymmetric plaque and may misidentify a plaque as two separate plaques when in reality there is only one plaque.

The novel semiautomated approach presented in this report allows plaque information to be obtained in a rapid and accurate manner, with minimal user interaction. As such, routine investigation could include systematic 3D data acquisition of the aorta during TEE imaging to improve the information on total aortic plaque burden in the echocardiographic report. Ideally, in the future, developments in this technology will allow 3D reconstruction of the entire thoracic aorta from 3D TEE data sets, with the integration of parametric display of plaque severity. This will allow standardization of analysis across echocardiography laboratories and provide quantification for reporting purposes, which aids in follow-up and use in clinical trials.

855 Finally, current evaluation of plaque severity is dependent on 2D
856 assessment of thickness or mobile components. However, although
857 increase plaque thickness is related to increased plaque volume, there
858 are plaques for which this relationship does not hold, and this explains
859 the weak correlation found between these two measurements in this
860 study. Theoretically, increased plaque volume should be a risk factor
861 for cardiovascular events. In fact, studies of carotid artery disease have
862 demonstrated that plaque volume is a stronger predictor of coronary
863 artery calcium than carotid intimal medial thickness.¹¹

864 One of the most important features of this new program is its
865 ability to quantify plaque volume from 3D aortic data sets in a semi-
866 automated way. This is a measurement that cannot be accurately
867 obtained from 2D data sets. The ability to acquire this measurement
868 from 3D data sets may improve the clinical quantification of aortic
869 atherosclerosis. Further studies are needed to determine the predic-
870 tive value of plaque volume and whether patients with significant
871 plaque volume and minimal thickening require aggressive manage-
872 ment.

876 Study Limitations

877 A limitation of this study is that the analysis was limited to the prox-
878 imal descending aorta, and thus the program's accuracy in the
879 ascending aorta and aortic arch was not demonstrated. However,
880 complex plaques are most commonly located in the proximal descen-
881 ding aorta, so it is the region where such a semiautomated
882 approach would be of most benefit. As well, 3D imaging of the aorta
883 only allows visualization in the far field of one-half to three-quarters of
884 the aortic circumference in each acquisition. When combined with
885 the spiral relationship to the descending thoracic aorta, the series of
886 3D aortic data sets only represents the far field descending aortic
887 wall—posterior aortic wall in the distal thoracic aorta, the lateral aortic
888 wall in the midthorax, and the anterior surface of the proximal descen-
889 ding aorta and arch. Thus, the entire descending aorta cannot
890 be visualized with 3D data sets.

891 Another limitation is that in its current form, the semiautomated
892 algorithm is focused on plaque segmentation and the computation
893 of thickness and volume only. Consequently, the scheme for plaque
894 severity does not take into account plaque ulceration or mobile com-
895 ponents. Thus, the current software algorithm may misinterpret an ul-
896 cerated plaque as a thin plaque.

897 Finally, the reference standard used in this study was 3D multiplanar
898 reconstruction rather than a different imaging modality. CT and
899 MRI are possible options. However, aortic CT is limited by the
900 need for contrast injection and exposure to radiation. Similarly,
901 MRI has limitations in that it cannot be performed at the bedside or
902 in patients with ferromagnetic implants, particles, or pacemakers.
903 The ultimate method to determine the true accuracy of this program
904 would be to perform a study with intraoperative or necropsy mea-
905 surements as the reference standard.

CONCLUSIONS

916 Semiautomated analysis for the detection and quantification of de-
917 scending aortic plaques from 3D TEE data sets is rapid, feasible,
918 and accurate in determining plaque severity as measured by plaque
919 thickness, volume, and number. This methodology allows the stan-
920 dardization of plaque quantification, which will improve its utility in
921 clinical trials. As well, this methodology introduces the ability to ac-
922 quire plaque volume measurements, which may play a role in the
923 assessment of disease severity.

REFERENCES

- 930 1. Hoyert DL, Xu J. Deaths: preliminary data for 2011. *Natl Vit Stat Rep* 2012;
931 61:1-64.
- 932 2. Douglas PS, Garcia MJ, Haines DE, Lai WW, Manning WJ, Patel AR, et al.
933 ACCF/AHA/ASNC/HFSA/HRS/SCAI/SCCM/SCCT/SCMR 2011
934 appropriate use criteria for echocardiography. A report of the American
935 College of Cardiology Foundation Appropriate Use Criteria Task Force,
936 American Society of Echocardiography, American Heart Association, Amer-
937 ican Society of Nuclear Cardiology, Heart Failure Society of America, Heart
938 Rhythm Society, Society for Cardiovascular Angiography and Interventions,
939 Society of Critical Care Medicine, Society of Cardiovascular Computed
940 Tomography, and Society for Cardiovascular Magnetic Resonance endorsed
941 by the American College of Chest Physicians. *J Am Coll Cardiol* 2011;57:
942 1126-66.
- 943 3. Amarenco P, Cohen A, Tzourio C, Bertrand B, Hommel M, Besson G, et al.
944 Atherosclerotic disease of the aortic arch and the risk of ischemic stroke. *N*
945 *Engl J Med* 1994;331:1474-9.
- 946 4. Tunick PA, Rosenzweig BP, Katz ES, Freedberg RS, Perez JL, Kronzon I.
947 High risk for vascular events in patients with protruding aortic atheromas:
948 a prospective study. *J Am Coll Cardiol* 1994;23:1085-90.
- 949 5. Kronzon I, Tunick PA. Aortic atherosclerotic disease and stroke. *Circula-*
950 *tion* 2006;114:63-75.
- 951 6. Lorensen WE, Cline HE. Marching cubes: a high resolution 3D surface
952 construction algorithm. *ACM SIGGRAPH Comput Graph* 1987;21:
953 163-9.
- 954 7. Khatri IA, Mian N, Alkawi A, Janjua N, Kirmani JF, Saric M, et al. Catheter-
955 based aortography fails to identify aortic atherosclerotic lesions detected
956 on transesophageal echocardiography. *J Neuroimaging* 2005;15:261-5.
- 957 8. Saric M, Kronzon I. Aortic atherosclerosis and embolic events. *Curr Car-*
958 *diol Rep* 2012;14:342-9.
- 959 9. Krinsky GA, Freedberg R, Lee VS, Rockman C, Tunick PA. Innominate ar-
960 tery atheroma: a lesion seen with gadolinium-enhanced MR angiography
961 and often missed by transesophageal echocardiography. *Clin Imaging*
962 2001;25:251-7.
- 963 10. Svedlund S, Wetterholm R, Volkmann R, Caidahl K. Retrograde blood
964 flow in the aortic arch determined by transesophageal Doppler ultrasound.
965 *Cerebrovasc Dis* 2009;27:22-8.
- 966 11. Sillesen H, Muntendam P, Adourian A, Entrekian R, Garcia M, Falk E, et al.
967 Carotid plaque burden as a measure of subclinical atherosclerosis: compar-
968 ison with other tests for subclinical arterial disease in the High Risk Plaque
969 Biolmage study. *JACC Cardiovasc Imaging* 2012;5:681-9.

APPENDIX

The algorithm was implemented using the open-source Insight Segmentation and Registration Toolkit and the Visualization Toolkit (<http://www.itk.org> and <http://www.vtk.org>), consisting of class libraries written in the C++ programming language. In particular, the former provides tools for segmenting and registering multidimensional images, while the latter uses algorithms for modeling and visualization.

Ideal Aortic Lumen Computation

Starting from the canonical equation of the ellipse,

$$dx^2 + exy + fy^2 + gx + hy + l = 0, \quad (\text{A1})$$

the ellipse center (c_x, c_y) , major (a) and minor (b) axis lengths, and ellipse orientation (ϑ) are identified using the least squares minimization criterion. Then, each point on the ellipse contour can be described by the following coordinates, through which the elliptical contour interpolating the five original points is generated:

$$x(t) = c_x + a \cos \vartheta \cdot \cos \phi - b \sin \vartheta \cdot \sin \phi, \quad (\text{A2})$$

$$y(t) = c_y + a \cos \vartheta \cdot \sin \phi + b \sin \vartheta \cdot \cos \phi. \quad (\text{A3})$$

Segmentation

On each aortic 2D cross-sectional cut plane in the volume of interest, the automated detection of the atheromas is performed by searching

in the corresponding cut plane of the mesh M the nodes (i.e., the vertices of the triangular patches constituting the mesh) that are inside the elliptical contour.

Given $m_i^n (x_i^n, y_i^n)$, the nodes of the mesh M in the n th cut plane, for each node the distance with the elliptical contour center (c_x^n, c_y^n) is computed as

$$\rho(m_i^n) = \sqrt{(c_x^n - x_i^n)^2 + (c_y^n - y_i^n)^2}, \quad (\text{A4})$$

together with its angular position θ_i^n with respect to a reference zero-degree orientation (see [Figure 3](#)).

On the basis of θ_i^n , the distance $r(\theta_i^n)$ between the corresponding point on the ideal aortic lumen elliptical contour and its center is computed as

$$r(\theta_i^n) = \frac{a^n \cdot b^n}{\sqrt{(b^n \cdot \cos(\theta_i^n))^2 + (a^n \cdot \sin(\theta_i^n))^2}}, \quad (\text{A5})$$

where a^n and b^n are the major and minor axes lengths of the n th ellipse. Finally, the comparison between $\rho(m_i^n)$ and $r(\vartheta_i^n)$ is performed:

- if $\rho(m_i^n) < r(\vartheta_i^n)$, the node m_i is classified as potential plaque, and the difference $r(\vartheta_i^n) - \rho(m_i^n)$ represents the local thickness;
- if $\rho(m_i^n) \geq r(\vartheta_i^n)$, the node m_i is classified as nonplaque.

Once this process has been repeated for all cut planes, the number of nodes for each resulting potential plaque is counted, and only plaques composed by >300 nodes (set empirically to avoid multiple small plaques due to possible noise in the mesh) are retained.

AUTHOR QUERY FORM

 ELSEVIER	Journal: YMJE Article Number: 3174	
--	---	--

Dear Author,

Please check your proof carefully and mark all corrections at the appropriate place in the proof (e.g., by using on-screen annotation in the PDF file) or compile them in a separate list. Note: if you opt to annotate the file with software other than Adobe Reader then please also highlight the appropriate place in the PDF file. To ensure fast publication of your paper please return your corrections within 48 hours.

For correction or revision of any artwork, please consult <http://www.elsevier.com/artworkinstructions>.

Any queries or remarks that have arisen during the processing of your manuscript are listed below and highlighted by flags in the proof.

Location in article	Query / Remark: Click on the Q link to find the query's location in text Please insert your reply or correction at the corresponding line in the proof
Q1 Q2 Q3 Q4	<p>If there are any drug dosages in your article, please verify them and indicate that you have done so by initialing this query</p> <p>Please provide professional degrees for all authors.</p> <p>Please disclose any conflict of interests or funding for this article.</p> <p>Please cite figure 3 after figure 2 citation in the text.</p> <p>Please confirm that given names and surnames have been identified correctly.</p> <div data-bbox="304 1332 895 1508" style="border: 1px solid black; padding: 5px;"> <p style="color: red;">Please check this box or indicate your approval if you have no corrections to make to the PDF file</p> <div style="display: inline-block; border: 1px solid black; width: 30px; height: 30px; vertical-align: middle;"></div> </div>

Thank you for your assistance.